Brain Stroke Lesion Segmentation Using Computed Tomography Images based on Modified U-Net Model with ResNet Blocks

https://doi.org/10.3991/ijoe.v18i13.32881

Azhar Tursynova[1], Batyrkhan Omarov[2(✉)], Aivar Sakhipov[3], Natalya Tukenova[4]
[1]Al-Farabi Kazakh National University, Almaty, Kazakhstan
[2]International University of Tourism and Hospitality, Turkistan, Kazakhstan
[3]Astana IT University, Nur-Sultan, Kazakhstan
[4]Zhetisu University named after I. Zhansugurov, Taldykorgan, Kazakhstan
batyahan@gmail.com

Abstract—Segmentation of brain regions affected by ischemic stroke helps to overcome the main obstacles in modern studies of stroke visualization. Unfortunately, contemporary methods of solving this problem using artificial intelligence methods are not optimal. Therefore, in the study we consider how to increase the efficiency of segmentation of the stroke focus using computer perfusion imaging using modifications based on UNet. The network was trained and tested using the ISLES 2018 dataset. The publication includes an analysis of the results obtained, as well as recommendations for future research. By choosing the appropriate model parameters, our approach can be easily applied to detect ischemic stroke. We present modified U-Net models with two ResNet blocks as U-Net+ ResNet-block 1 and U-Net +ResNetblock 2, as well as a modified UNet model. Due to the small number of images for training the model, the best results were obtained by applying data preprocessing and object representation approaches, as well as data normalization methods to avoid overfitting. The results show that the modified UNet model is superior to other models in terms of average distance and recall, that are significant parameters for segmentation of the stroke.

Keywords—brain stroke, deep learning, U-Net, computed tomography, segmentation

1 Introduction

Stroke ranks third among the most prevalent causes of mortality after cardiovascular stroke disease and newborn diseases [1]. Cerebral hypoxia occurs when the brain's cells reduce their ability to get oxygen as a consequence of a reduced or entirely interrupted blood flow. This results in the loss of brain cells in a short period of time. Stroke may be classified into several categories as ischemic stroke, hemorrhagic stroke, and spinal stroke. It is estimated that ischemia accounts for approximately 87% of stroke cases [2], and it is impacted by a reducing of blood flow which can lead to the death of the tissue. Other types of stroke are hemorrhagic in nature, and they are caused by the bursting of a vessel within the brain. Because of the pressure exerted by the leaking

blood, brain cells are damaged in this situation. Despite the fact that hemorrhagic stroke is a less frequent occurrence, it is associated with a high death rate [3]. Early stroke detection is associated with a better patient prognosis, and so time is critical in achieving a good treatment result for stroke. Hence, prompt clinical intervention is essential in order to provide the patient with the best suitable therapy.

For stroke diagnosis, the most widely employed imaging techniques are computed tomography (CT) and magnetic resonance imaging (MRI). CT scans are the most commonly used technique for the diagnostics of intraventricular hemorrhage [4]. All patients may benefit from CT scans since they are generally accessible, affordable and quick. In most cases, when a patient arrives at the hospital, CT scanning is the first neuroimaging procedure conducted. As a result, magnetic resonance imaging (MRI) may be utilized to diagnose various classes of hemorrhages.

Deep learning techniques have been applied in a variety of disciplines, with convolutional neural network (CNN) based systems showing outstanding results in digital image processing comparing to prior-scheme performance [5–7]. By using an encoder-decoder architecture and a skip-connection technique, U-Net [8] may minimize the loss of background and specific details. Consequently, U-Net is useful for image segmentation processes that need a moderate quantity of data, and it has shown high efficiency in working with medical images [9–10] and other applications. Kadry et al. [11] conducted an investigation on brain stroke segmentation using a Visual Geometry Group UNet (VGG-UNet). It does, however, need a large number of nodes in the input layer due to the fact that it performs repeating convolution operations for feature engineering. Aside from that, it's indeed challenging to segment stroke lesions of varying sizes and locations due to long-term reliance difficulties, such as the limited efficiency of feature reusability, which make segmenting lesions of varying sizes and locations problematic.

U-Net is regarded as one of the most effective models for segmenting medical imagery. We proposed comparison of the integrated U-Net models with ResNetblock1, ResNetblock2, and an improved UNet for brain stroke segmentation using CT images in this article. The data augmentation strategy was adopted in the research since the quantity of data for training was restricted. After removing the object, the segmentation step is conducted in the major section. We used four key assessment criteria to achieve the results: Intersection of Units (IoU), dice similarity coefficient (DSC), F-measure, and accuracy. In comparison to the combined UNet+ResNet blocks, the improved UNet model segments cerebral stroke with a high performance of stroke lesion segmentation.

2 Related works

In the 1970s and 1990s, medical pictures were analyzed using sequential low-level pixel processing and computational analysis [12]. Some prior researches have included typical machine learning techniques as well as handcrafted attributes to increase the performance of brain stroke lesion segmentation. Whereas texture-based characteristics, such as angles, borders, et cetera, may be used to improve segmentation performance [13], they are not the most effective way to detect ischemic strokes, since stroke lesions exist in a wide range of sizes and forms [14].

Deep learning techniques have shown to be quite useful in studies using brain magnetic resonance imaging (MRI) data. To identify low-quality photos in a database of

1000 participants, Sujit et al. developed a basic CNN. For the detection of low-quality imagery data, Fantini et al. highlighted using the Inception design on image regions from several orientations of slices [15], which they described as follows: according to Shaw et al. [16], it is possible to construct artefact pictures of brain MRI in order to enhance the training process and reduce the dependence of accuracy on visual acuity. The majority of the work has been on picture artifact identification and its effect on regression tasks, although this has not been examined in depth to yet. Artefact repair has not gotten the same amount of attention from the community as picture artefact identification, and there are only a small number of research on correction using deep learning models [17] that have been published so far. Among the many shortcomings of the existing research is the absence of an investigation of the effect of picture artefacts on segmentation, which we address in more depth in this study. The limited number of artefact correction techniques, as well as the prevalent practice of deleting low-quality photos in observational studies, are two further issues to be concerned about. In contrast, the existing work concentrates on specific concerns such as artefact identification, correction, and post-processing in isolation, undermining the value of picture quality in population investigations.

A 3D fully CNN was built by Zhang et al. [18] to divide ischemic stroke lesions from image captured by diffusion-weighted imaging (DWI). Nevertheless, whereas a 3D CNN has many more properties than a 2D CNN, developing 3D CNNs is more challenging and requires extra data to train. As a consequence, 3D patches has been used to train spatial classifiers or straight images, which might lead to data leakage and challenges with zero derivative. Deep residual CNN approach was constructed by Liu et al. [19] to categorize acute ischemic strokes employing multimodality MRI. It leverages multimodality to capture complementary data in MRIs and combines a residual unit into a U-shaped model, which may enhance segmentation quality by increasing the quantity of data accessible to the method. Liu et al. [20] developed a novel neural network that uses rectified linear unit (ReLU) activation in the last two layers to achieve accurate reconstruction of the stroke lesion during ischemic stroke modeling. The lack of lightweight trainable models necessitates speed, and the network is incapable of capturing the non-linear link between features, making it insufficient. Karthik et al. [21] proposed a fully convolutional neural network for segmenting stroke lesions on MRI. Guerrero and colleagues [22] have proposed u-ResNet, a 2D U-shaped residual neural network for lesion segmentation. The aforementioned approaches can also benefit from the ability to exploit data at large global scales without losing valuable specific information. The technique proposed in this study may be consistent with current methods.

3 Materials and methods

The UNet structure for cell segmentation on microscopy images, created by Olaf Ronneberger et al. 2015, has given positive results and is frequently utilized to tackle image segmentation challenges [24]. This design is composed of two components: an encoder and a decoder, which together create a U-design [25]. The picture goes through a sequence of layers at the input in the narrowing half of the structure: convolutional layers with combination layers. The traditional UNet design is shown in Figure 1.

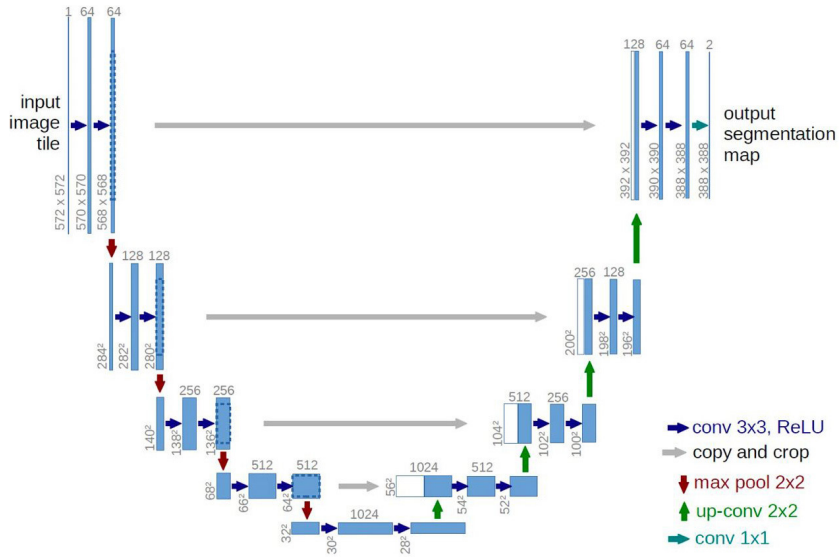

Fig. 1. Classical UNet model [26]

The Residual Network, abbreviated ResNet, was created in 2015 by Microsoft Research scientists. The main task of ResNet was to solve the problem of disappearing or exploding gradient,. The basic concept in the ResNet architecture is residual blocks, as well as the method of skipping connections. The method of skipping connections, as the name itself says, connects activation layers with other layers by passing some layers between them, thereby forming a residual block. Stacking the residual blocks together and creating re-connections. The main focus of the ResNet network is to match the residual mapping instead of studying the networks to the basic mapping. The ResNet architecture consists of 34 layers, stimulated by VGG-19, where a fast connection is added after. Thanks to fast connections, the architecture is then transformed into a residual network. The ResNet architecture is presented in Figure 2.

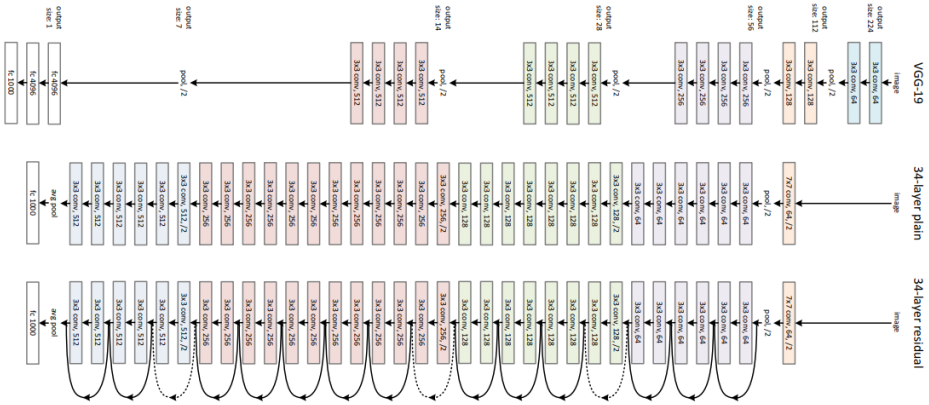

Fig. 2. ResNet architecture [27]

3.1 Math description

In this study, we Input a CT image into the network. So, *Input* (C_{in}, D_{in}, H_{in}, W_{in}) is 3D convolution. Here, *W* stands for weight, *H* stands for height, *D* stands for depth, *C* is card of objects.

Thus, equation (1) means 3D convolution operation.

$$Y_{i,k,x,y,z} = \sum_{c=0}^{C-1} \sum_{t=0}^{T-1} \sum_{r=0}^{R-1} \sum_{s=1}^{S-1} I_{i,c,x+t,y+r,z+s} F_{k,t,r,s,c} \tag{1}$$

Here, $Y_{i,k,x,y,z}$ is a result of the convolution, $I_{i,c,x+t,y+r,z+s}$ is an input object, $F_{k,t,r,s,c}$ is a filter.

Next method that we apply to UNet is L2 regularization. Equation (2) shows the meaning of this method.

$$\sum_{i=0}^{N} \left(y_i - \sum_{j=0}^{M} x_{ij} W_j \right)^2 + \lambda \sum_{j=0}^{M} W_j^2 \tag{2}$$

Here, *n* is dimension of y_i and x_i. λ is a regularization parameter.

Next method is a normalization of instance.

$$\mu_{ni} = \frac{1}{HW} \sum_{l=1}^{W} \sum_{m=1}^{H} x_{nilm} \tag{3}$$

$$\delta_{ni}^2 = \frac{1}{HW} \sum_{l=1}^{W} \sum_{m=1}^{H} (x_{nilm} - \mu_{ni})^2 \tag{4}$$

Here, *x* is a tensor, *N* is an image package.

Equation (5) means normalization of input images.

$$y_{nijk} = \frac{x_{nijk} - \mu}{\sqrt{\sigma_{ni}^2 + \varepsilon}} \tag{5}$$

ε is a small added value for more stable learning.

We also utilize dropout to avoid complicated coadaptations of individual neurons on training data, which reduces network overfitting. Equation (6) demonstrates dropout process.

$$y = f(Wx) \circ m, \quad m_i \sim \text{Bernoulli}(p) \tag{6}$$

Here, *p* is dropout. $y = (1-p) f(Wx)$ is a test stage.

Thus, in this section, we explained mathematical representations of the proposed techniques. The following section contains an explanation of evaluation metrics for assessment of the proposed system in stroke diagnosis.

3.2 Dataset

The ISLES Challenge 2018 dataset [23] was applied to train and validate the proposed approach based on U-shaped network with ResNet blocks. As input data for the models, 3D images are used, which consist of 6 types. Cerebral blood flow (CBF), Cerebral blood volume (CBV), Mean transit time (MTT), Time-to-Maximum (Tmax) and cerebral vascular mean transit time (MTT) are all included in this dataset, as well as baseline 4D Computed Tomography Perfusion (4D CTP) scanning and 3D Computed Tomography Perfusion (3D CTP) maps. Then, within 3 hours of the baseline CTP scanning, each patient got a diffusion-weighted magnetic resonance imaging (DW-MRI) to confirm the results. The DW-MRI images were tagged by a specialist in order to trace the real brain ischemic stroke lesion. The dataset contains data for 103 patients, with 63 people being the training set and 40 people representing the test set. The training and test sets each include 94 and 62 images, respectively. Figure 3 demonstrates samples of a set of input data for stroke lesions segmentation.

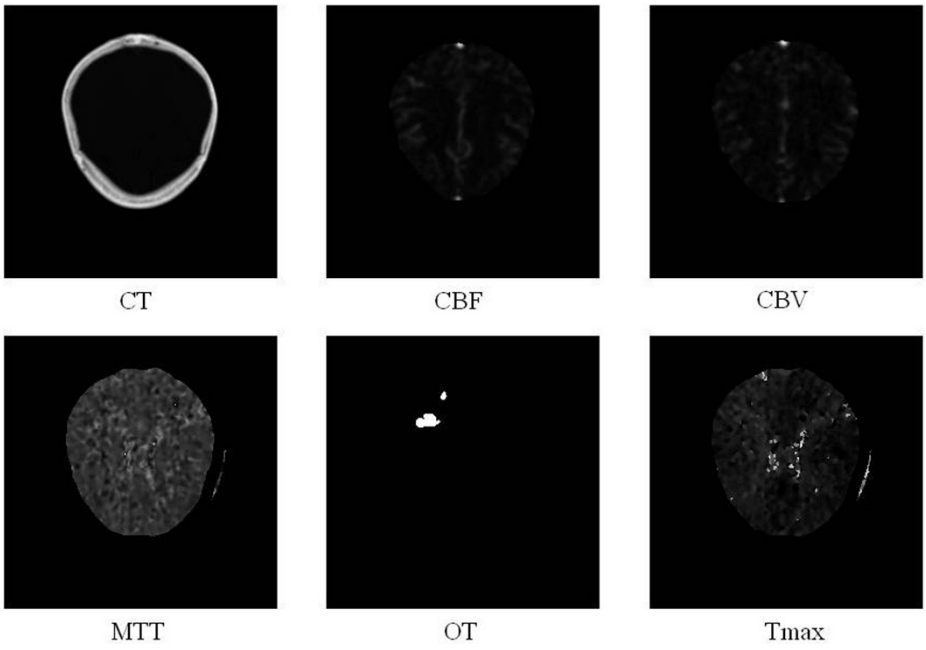

Fig. 3. Sample of ISLES 2018 dataset for stroke lesion segmentation

3.3 Evaluation metrics

Evaluation criteria include Dice, Hausdorff Distance, Average Distance, Precision, Recall, and Average Distance. In this section, we explain each of the evaluation parameters that applied in current research.

The Dice similarity coefficient or Jaccard similarity coefficient are used in network training to display a measure of similarity. The example below illustrates the area of properly tagged segments. The dice similarity coefficient is shown in Equation (7) [46].

$$Dice(A,B) = \frac{2|A \cap B|}{|A| + |B|} \tag{7}$$

Here, A and B are sets. A is a ground truth of the stroke lesions; B is a predicted volume of stroke lesions. In the best case, when predicted value coincides with the ground truth, then dice = 1. In the worst case, when predicted value does not intersect with the ground truth, then dice = 0.

Jacquard similarity is a simple but sometimes powerful similarity metric. Two sequences A and B are given: we find the number of common elements in them and divide the found number by the number of elements of both sequences. Equation (8) demonstrates Jaccard similarity index for stroke segmentation [28].

$$J(A,B) = \frac{|A \cap B|}{|A \cup B|} \tag{8}$$

Precision efficiently reflects the purity of positive detections when compared to the actual data. How many of the items in a given picture that we anticipated had a matching ground truth annotation? Precision is described by Equation (9) [29].

$$precision = \frac{TP}{TP + FP} \tag{9}$$

Here, TP is true positives, FP is false positives.

The validity of our optimistic predictions in relation to the ground truth is efficiently described by recall. How many positive predictions have we received from all the objections in our basic truth? [30]

$$recall = \frac{TP}{TP + FN} \tag{10}$$

Here, TP means true positive values; FN is false negative values that were obtained during the model testing.

4 Experiment results

In this study, methods of combination and modification of UNet models were used to improve the performance of stroke segmentation on CT images. As an experiment, we combined the UNet model with ResNetblock_1 and ResNetblock_2, and also modified the U-Net model itself. The combination in the UNet+ResNetblock_1 architecture, brought the total number of parameters to 4,382,949, of which the trainable parameters were 4,379,621, while the non-trainable parameters were 3,328. In this experiment, the ResNet block was added to the part of the deconvolution of the UNet architecture. In the following experiment, UNet+ResNetblock_2 batch normalization was performed after each 3D convolution block, the ResNet block was added to the convolution of a part of the UNet architecture. There were only 8,921,641 parameters in this model, of which 8,921,509 were trainable and only 132 were unprepared. Thus, it has been established

that each time the number of unprepared parameters decreases. In the third UNet architecture, several changes were made such as instance normalization and re-leakage. The number of common and trainable parameters was greater than that of the first two – 16,321,121, and as a result, the number of untrained parameters was – 0. We were also able to adapt the original 3D UNet using Adam optimizer, data dropout, data augmentation process, L2 regularization methods.

We propose a modification of UNet that benefits of each strategies that listed below:

- Data augmentation. Developers may use this strategy to artificially expand the size of the training set by changing an original dataset [31–32]. This approach was chosen for training since the applied dataset included a little quantity of data.
- Dropout was created to address the issue of having to re-adjust the weights during testing owing to a high number of parameters [33s].
- The Adam optimization approach improves adaptive learning performance. It was created with deep neural network training in mind [34].
- By restricting the coefficient and conserving all variables, L2 regularization overcomes multicollinearity concerns [35].
- Instance Normalization eliminates changes in the mean and covariance for a single instance, making the learning process accessible. In a job like picture style, the normalizing procedure permits the elimination of information about a specific instance's contrast from the content image, which simplifies creation [36].

During the training of the models, the results of training and validation losses were obtained in the form of a linear graph, which are shown in Figure 4.

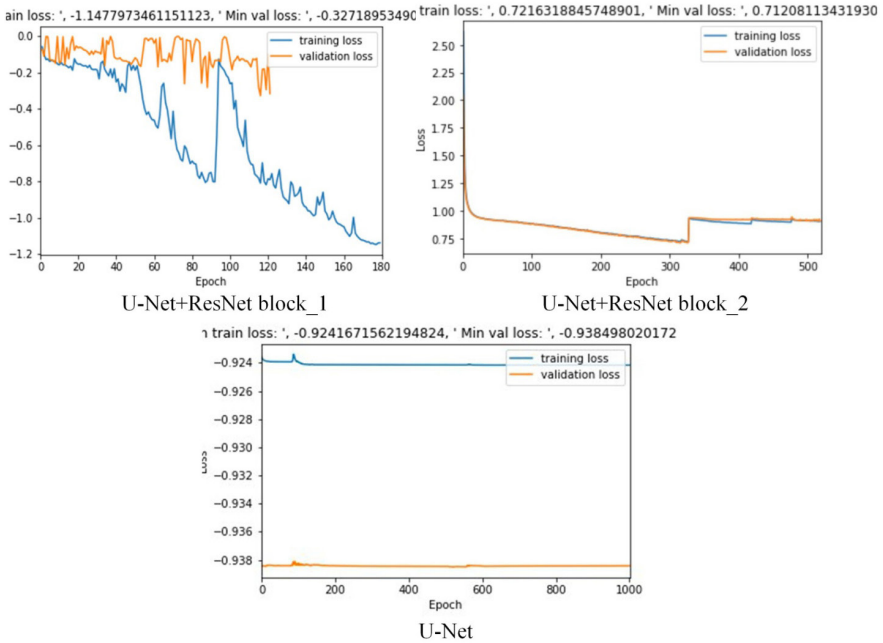

Fig. 4. Training and validation loss results of three models (U-Net+ResNetblock_1, U-Net+ResNetblock_2 and U-Net)

The result is obtained by sending the received test results to the SMIR database [37]. Table 1 shows the results of each model obtained from our experiments that evaluated by different metrics as Dice similarity coefficient, Hausdorff Distance, Average Distance, Precision, Recall and AVD. As it can be noticed from Table 1, U-Net model with ResNet Blocks_2 demonstrates higher results in majority of the parameters (Dice, Husdorff distance, Recall, AVD) than the other models including the classical U-Net. The obtained results prove the efficiency of the proposed technique.

Table 1. Comparative results for each model

Model	Dice	Hausdorff Distance	Average Distance	Precision	Recall	AVD
U-Net+ResNet block_1	0.09	19354907.28	19354854.75	0.06	0.25	34.93
U-Net+ResNet block_2	0.30	19354903.82	19354854.08	0.24	0.33	45.85
U-Net	0.21	19354901.36	19354848.45	0.26	0.25	19.23

Further, we demonstrate segmentation results of the applied U-Net modifications. Figures 5, 6, 7 presents the comparative results of the original drawings of the foci of stroke segmentation and predicted results.

As can be seen in Figure 5, segmented stroke foci using UNet+ResNetblock_1 gave an inaccurate result.

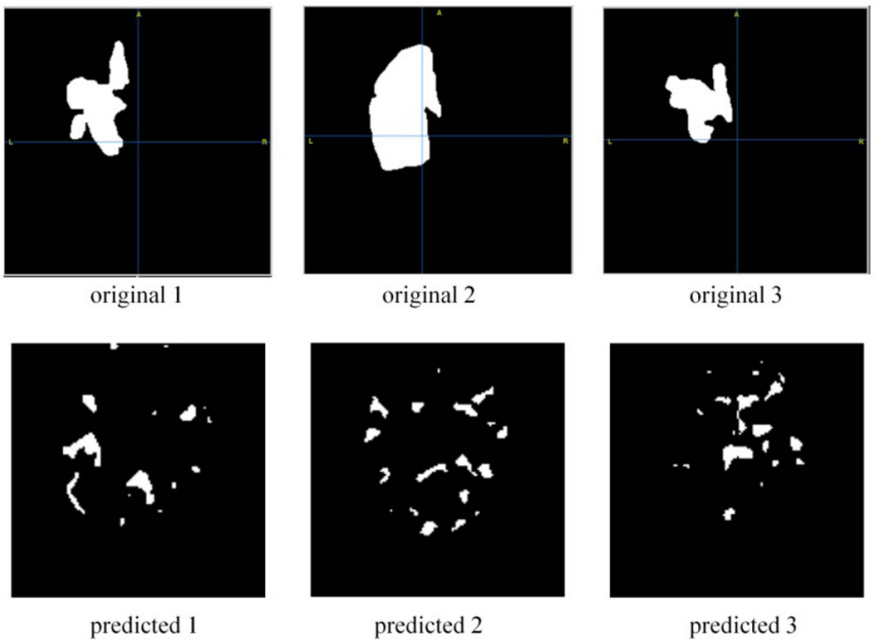

Fig. 5. Predicted results of stroke segmentation on U-Net+ResNet block_1 model

Figure 6 demonstrates segmentation results of the proposed U-Net model with ResNet block_2 for three cases.

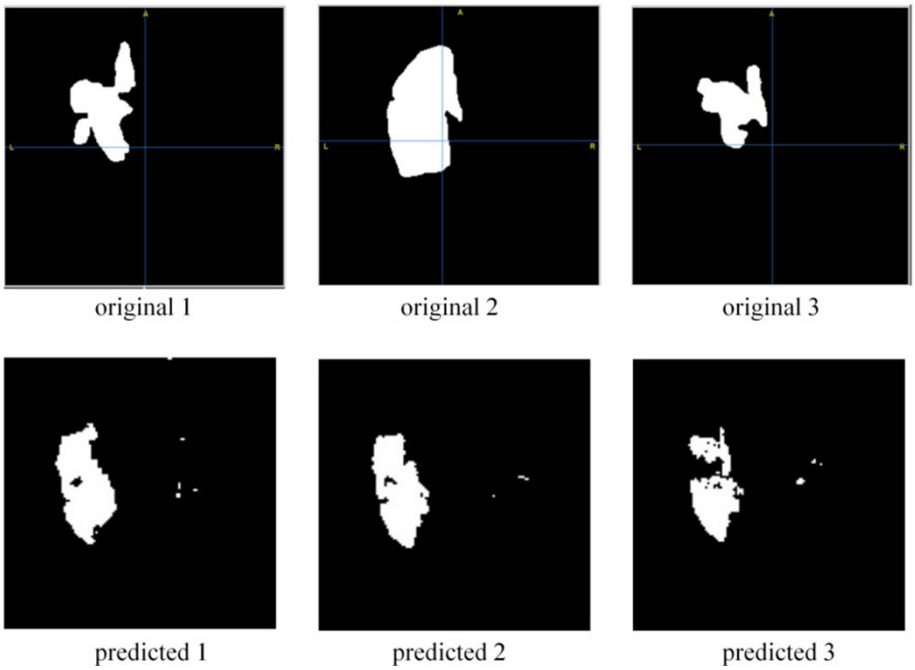

Fig. 6. Predicted results of stroke segmentation on U-Net+ResNet block_2 model

Figure 7 demonstrates stroke segmentation results when using classical U-Net. As a result of the experiment, it turned out that with regards to both the first and second cases, the application of ResNet blocks gave a low result compared to the modified U-Net. Thus, we have identified that combining blocks of different models is less efficient than using a completely separate model, such as in our case of a modified U-Net.

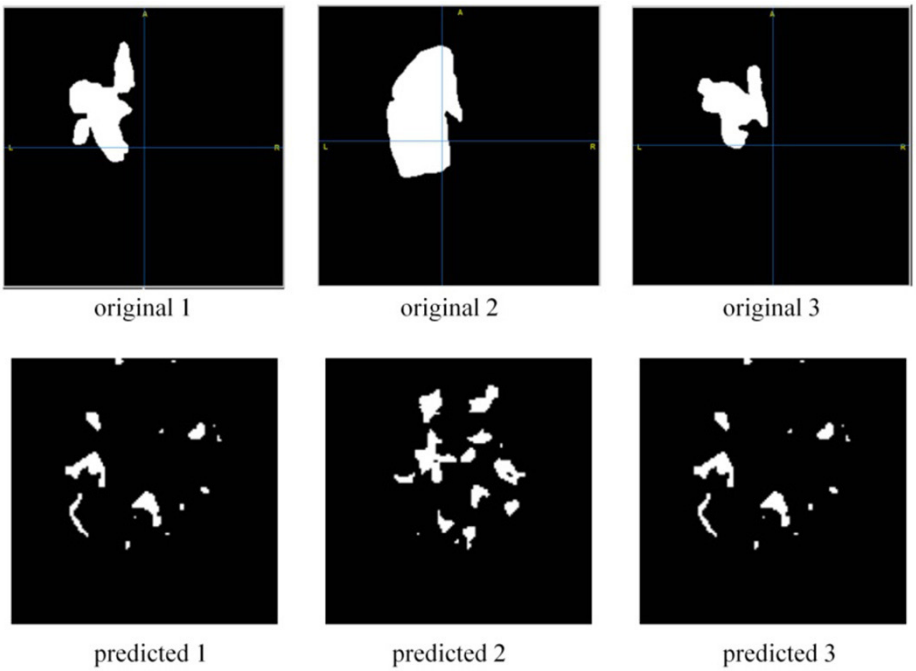

Fig. 7. Predicted results of stroke segmentation on U-Net model

During the training of each model (UNet+Resetblock_1, UNet+Resetblock_2 and U-Nat), an early stop method was applied to prevent learning problems. Incorrect determination of the required number of epochs can lead to overfitting of the training dataset, while too little can lead to insufficient fitting of the model. The use of the early stop method will allow you to determine the exact number of epochs. Initially, an epoch of 10000 was set arbitrarily for all models, but when training, the early stop method stopped training as soon as the performance of the models stopped improving in the data set for checking the delay. Thus, the schedule of loss of training and validation differs for each module in its own way.

5 Discussion

The implementation of recommendation systems into clinical research is a critical undertaking that will substantially quicken and improve the efficacy of therapeutic treatment for cerebral cerebrovascular accident. Automated classification and processing of neuroimages will enable rapid differentiated diagnostics, prediction of likely disease outcomes, and personalized recommendations for one of the most vital therapeutic option for patients. The availability of a representative group comprised of a significant quantity of organized and accurate data serves as the foundation for implementing different techniques of computer – aided diagnosis,

incorporating cognitive computing and artificial intelligence. The algorithms' efficacy and performance are also closely related to the quality of the original data or training set and need meticulous pre-processing [38].

During the research it is essential to look for instances that satisfy the following conditions within specific hospitals of a local repository, proceeded by a time-consuming procedure of manually tagging the photos by specialists. This is why learning items often comprise just under one hundred diagnostic tests [39].

In spite of the importance of automated systems of identifying and treating strokes, the global availability of suitable image files in open access is limited, and in many regions of the world, such developments are entirely absent, inherently resulting in a loss of accuracy of models constructed using open statistical data. The primary goal of establishing open datasets is to aid teams in enhancing and managing methodologies for fully automated lesion detection and segmentation. Frequently, samples are addressed with clinical criteria for cerebrovascular disease [39–41] or images with established huge regions of ischemia, and contain insufficient clinical data from the patient. Certain samples do not contain lesions or are segmented automatically without the involvement of specialists, making their being used as a training instances difficult without initial data processing. Without a reason to suspect, early identification of patient populations with artificial intelligence are critical, but data enabling its construction are scarce at the time. Furthermore, large-scale projects devoted entirely to cerebral ischemia tumors, such as ENIGMA Stroke Recovery [42], ATLAS [43], ISLES contest [23], all of which took place between 2016 and 2018, simply focus on MRI collection and that certain types of underlying neural studies. While images from these technologies are obviously very valuable for medical decision, the technologies themselves are not frequently employed for stroke diagnosis. Another frequent problem of public access picture collections is their compression or preceding the formats that sacrifice quality and information, greatly limiting investigators' technique selection.

6 Conclusion

Brain image classification and segmentation is still a work in progress in the realm of deep learning. In image segmentation, the number of accessible materials in the research is also significant. We suggested coupled and modified UNet models with ResNet blocks for segmenting brain stroke lesion in this paper. In turn, the UNet model is one of the most effective approaches for segmenting medical imaging when used to small datasets. Furthermore, one of the experimental models assisted in enhancing the precision of computed tomography image segmentation, resulting in improved outcomes. The best model we presented during the investigation reached a 31 percent dice coefficient and a 35 percent recall/sensitivity, demonstrating the accurateness of the technological advances used to improve the classical 3D UNet. We plan to improve the leader model in the future by using fine-tuning and extraction functions. It's also meant to construct our own weighting factors, which will help us enhance the proposed model by setting layers with the most abstractions, and object extraction will be used in the future for even more effective ones. As a result, we expect that using these

techniques will improve the accuracy and precision of the assessment criteria, bringing the segmentation process closer to highly accurate.

7 Data availability

We utilize the ISLES 2018 open dataset for this investigation, which was created as a part of a medical picture segmentation challenge [44–45]. http://www.isles-challenge.org/ provides access to the dataset.

8 References

[1] Aked, J., Delavaran, H., & Lindgren, A. G. (2021). Survival, causes of death and recurrence up to 3 years after stroke: A population-based study. European Journal of Neurology, 28(12), 4060–4068. https://doi.org/10.1111/ene.15041

[2] Zhao, L., Cao, S., Pei, L., Fang, H., Liu, H., Wu, J., … & Xu, Y. (2022). Validation of CSR model to predict stroke risk after transient ischemic attack. Scientific Reports, 12(1), 1–8. https://doi.org/10.1038/s41598-021-04405-2

[3] Liddle, L. J., Kalisvaart, A. C., Abrahart, A. H., Almekhlafi, M., Demchuk, A., & Colbourne, F. (2022). Targeting focal ischemic and hemorrhagic stroke neuroprotection: Current prospects for local hypothermia. Journal of Neurochemistry, 160(1), 128–144. https://doi.org/10.1111/jnc.15508

[4] Theologou, M., Natsis, K., Kouskouras, K., Chatzinikolaou, F., Varoutis, P., Skoulios, N., … & Tsonidis, C. (2022). Cerebrospinal fluid homeostasis and hydrodynamics: A review of facts and theories. European Neurology, 1–13. https://doi.org/10.1159/000523709

[5] Ahmed, S. T., & Kadhem, S. M. (2021). Using machine learning via deep learning algorithms to diagnose the lung disease based on chest imaging: A survey. International Journal of Interactive Mobile Technologies, 15(16). https://doi.org/10.3991/ijim.v15i16.24191

[6] Nuanmeesri, S. (2022). Feature selection for analyzing data errors toward development of household big data at the sub-district level using multi-layer perceptron neural network. International Journal of Interactive Mobile Technologies, 16(5). https://doi.org/10.3991/ijim.v16i05.22523

[7] Chan, S., Huang, C., Bai, C., Ding, W., & Chen, S. (2022). Res2-UNeXt: A novel deep learning framework for few-shot cell image segmentation. Multimedia Tools and Applications, 81(10), 13275–13288. https://doi.org/10.1007/s11042-021-10536-5

[8] Siddique, N., Paheding, S., Elkin, C. P., & Devabhaktuni, V. (2021). U-Net and its variants for medical image segmentation: A review of theory and applications. IEEE Access. https://doi.org/10.1109/ACCESS.2021.3086020

[9] Samann, F. E., Abdulazeez, A. M., & Askar, S. (2021). Fog computing based on machine learning: A review. International Journal of Interactive Mobile Technologies, 15(12). https://doi.org/10.3991/ijim.v15i12.21313

[10] Kaur, A., Kaur, L., & Singh, A. (2021). GA-UNet: UNet-based framework for segmentation of 2D and 3D medical images applicable on heterogeneous datasets. Neural Computing and Applications, 33(21), 14991–15025. https://doi.org/10.1007/s00521-021-06134-z

[11] Kadry, S., Damaševičius, R., Taniar, D., Rajinikanth, V., & Lawal, I. A. (2021, March). U-Net supported segmentation of ischemic-stroke-lesion from brain MRI slices. In 2021 Seventh International Conference on Bio Signals, Images, and Instrumentation (ICBSII) (pp. 1–5). IEEE. https://doi.org/10.1109/ICBSII51839.2021.9445126

[12] Abdelrahman, A., & Viriri, S. (2022). Kidney tumor semantic segmentation using deep learning: A survey of state-of-the-art. Journal of Imaging, 8(3), 55. https://doi.org/10.3390/jimaging8030055

[13] Mikes, S., & Haindl, M. (2021). Texture segmentation benchmark. IEEE Transactions on Pattern Analysis and Machine Intelligence. https://doi.org/10.1109/TPAMI.2021.3075916

[14] Lee, S., Low, C. Y., Kim, J., & Teoh, A. B. J. (2022). Robust sclera recognition based on a local spherical structure. Expert Systems with Applications, 189, 116081. https://doi.org/10.1016/j.eswa.2021.116081

[15] Sujit, S. J., Gabr, R. E., Coronado, I., Robinson, M., Datta, S., & Narayana, P. A. (2018, December). Automated image quality evaluation of structural brain magnetic resonance images using deep convolutional neural networks. In 2018 9th Cairo International Biomedical Engineering Conference (CIBEC) (pp. 33–36). IEEE. https://doi.org/10.1109/CIBEC.2018.8641830

[16] Shaw, R., Sudre, C., Ourselin, S., & Cardoso, M. J. (2018, December). MRI k-space motion artefact augmentation: Model robustness and task-specific uncertainty. In International Conference on Medical Imaging with Deep Learning – Full Paper Track.

[17] Wang, M., Xu, Z., Liu, X., Xiong, J., & Xie, W. (2022). Perceptually quasi-lossless compression of screen content data via visibility modeling and deep forecasting. IEEE Transactions on Industrial Informatics. https://doi.org/10.1109/TII.2021.3139895

[18] Zhang, Y., Wu, J., Liu, Y., Chen, Y., Chen, W., Wu, E. X., … & Tang, X. (2021). A deep learning framework for pancreas segmentation with multi-atlas registration and 3D level-set. Medical Image Analysis, 68, 101884. https://doi.org/10.1016/j.media.2020.101884

[19] Liu, J., Zhang, W., Tang, Y., Tang, J., & Wu, G. (2020). Residual feature aggregation network for image super-resolution. In Proceedings of the IEEE/CVF conference on computer vision and pattern recognition (pp. 2359–2368). https://doi.org/10.1109/CVPR42600.2020.00243

[20] Liu, C., Pang, F., Liu, Y., Liang, K., Li, X., Zeng, X., & Ye, C. (2020, April). Semi-supervised brain lesion segmentation using training images with and without lesions. In 2020 IEEE 17th International Symposium on Biomedical Imaging (ISBI) (pp. 279–282). IEEE. https://doi.org/10.1109/ISBI45749.2020.9098565

[21] Karthik, R., Gupta, U., Jha, A., Rajalakshmi, R., & Menaka, R. (2019). A deep supervised approach for ischemic lesion segmentation from multimodal MRI using fully convolutional network. Applied Soft Computing, 84, 105685. https://doi.org/10.1016/j.asoc.2019.105685

[22] Guerrero, R., Qin, C., Oktay, O., Bowles, C., Chen, L., Joules, R., et al. White matter hyperintensity and stroke lesion segmentation and differentiation using convolutional neural networks NeuroImage, Clin., 17 (Jan. 2018), pp. 918–934. https://doi.org/10.1016/j.nicl.2017.12.022

[23] ISLES: Ischemic Stroke Lesion Segmentation Challenge, 2021. [Online]. Available: http://www.isles-challenge.org/

[24] Wang, Y., Katsaggelos, A. K., Wang, X., and Parrish, T. B. (2016). A deep symmetry convnet for stroke lesion segmentation. In 2016 IEEE International Conference on Image Processing (ICIP), Phoenix, AZ, USA, pp. 111–115. https://doi.org/10.1109/ICIP.2016.7532329

[25] Liu, L., Cheng, J., Quan, Q., Wu, F. X., Wang, Y. P., & Wang, J. (2020). A survey on U-shaped networks in medical image segmentations. Neurocomputing, 409, 244–258. https://doi.org/10.1016/j.neucom.2020.05.070

[26] U-Net: Convolutional networks for biomedical image segmentation, 2021. [Online]. Available: https://lmb.informatik.uni-freiburg.de/people/ronneber/u-net/

[27] He, K., Zhang, X., Ren, S., and Sun, J. (2016). Deep residual learning for image recognition, in Proceedings of the IEEE conference on computer vision and pattern recognition, Las Vegas, NV, USA, pp. 770–778. https://doi.org/10.1109/CVPR.2016.90

[28] Omarov, B., Tursynova, A., Postolache, O., Gamry, K., Batyrbekov, A., Aldeshov, S., … & Shiyapov, K. (2022). Modified U net model for brain stroke lesion segmentation on computed tomography images. CMC-Computers Materials & Continua, 71(3), 4701–4717. https://doi.org/10.32604/cmc.2022.020998

[29] Omarov, B., Saparkhojayev, N., Shekerbekova, S., Akhmetova, O., Sakypbekova, M., Kamalova, G., … & Akanova, Z. (2022). Artificial intelligence in medicine: Real time electronic stethoscope for heart diseases detection. CMC-Computers Materials & Continua, 70(2), 2815–2833. https://doi.org/10.32604/cmc.2022.019246

[30] Natu, M., Bachute, M., Gite, S., Kotecha, K., & Vidyarthi, A. (2022). Review on epileptic seizure prediction: Machine learning and deep learning approaches. Computational and Mathematical Methods in Medicine, 2022. https://doi.org/10.1155/2022/7751263

[31] Data augmentation in Python: Everything you need to know, 2021. [Online]. Available: https://neptune.ai/blog/data-augmentation-in-python

[32] Fejer, H. N., Hasan, A. H., & Sadiq, A. T. (2022). A survey of toulmin argumentation approach for medical applications. International Journal of Online & Biomedical Engineering, 18(2). https://doi.org/10.3991/ijoe.v18i02.28025

[33] Srivastava, N., Hinton, G., Krizhevsky, A., Sutskever, I., and Salakhutdinov, R. (2014). Dropout: A simple way to prevent neural networks from overfitting. The Journal of Machine Learning Research, vol. 15, pp. 1929–1958. 10.5555/2627435.2670313

[34] Adam – latest trends in deep learning optimization, 2018. [Online]. Available: https://towardsdatascience.com/adam-latest-trends-in-deep-learning-optimization-6be9a291375c

[35] L2 and L1 regularization in machine learning, 2021. [Online]. Available: https://www.analyticssteps.com/blogs/l2-and-l1-regularization-machine-learning

[36] Ulyanov, D., Vedaldi, A., and Lempitsky, V. Instance normalization: The missing ingredient for fast stylization, arXiv preprint arXiv:1607.08022, 2016.

[37] Gerber, N., Reyes, M., Barazzetti, L., Kjer, H. M., Vera, S., Stauber, M., Mistrik, P., Ceresa, M., Mangado, N., Wimmer, W., et al. A Multiscale Imaging and Modelling Dataset of the Human Inner Ear. Sci. Data. 2017, 4, 170132. https://doi.org/10.1038/sdata.2017.132

[38] Chilamkurthy, S., Ghosh, R., Tanamala, S., Biviji, M., Campeau, N. G., et al. Development and validation of deep learning algorithms for detection of critical findings in head CT scans, arXiv preprint arXiv:1803.05854, 2018. [Online]. Available: https://arxiv.org/abs/1803.05854; https://doi.org/10.1016/S0140-6736(18)31645-3

[39] Pandian, J. D., Kalkonde, Y., Sebastian, I. A., Felix, C., Urimubenshi, G., et al. (2020). Stroke systems of care in low-income and middle-income countries: Challenges and opportunities, The Lancet, vol. 396, no. 10260, pp. 1443–1451. https://doi.org/10.1016/S0140-6736(20)31374-X

[40] M. Hssayeni. Computed tomography images for intracranial hemorrhage detection and segmentation (version 1.3.1), PhysioNet, 2020, 10.13026/4nae-zg36

[41] Gautam, A., and Raman, B. Towards effective classification of brain hemorrhagic and ischemic stroke using CNN. Biomedical Signal Processing and Control, vol. 63, pp. 102178, 2021. https://doi.org/10.1016/j.bspc.2020.102178

[42] Enigma stroke recovery, 2021. [Online]. Available: http://enigma.ini.usc.edu/ongoing/enigma-stroke-recovery/

[43] Liew, S. L., Anglin, J. M., Banks, N. W., Sondag, M., Ito, K. L., et al. (2018). A large, open source dataset of stroke anatomical brain images and manual lesion segmentations. Scientific Data, vol. 5, no. 1, pp. 1–11. https://doi.org/10.1038/sdata.2018.11

[44] Grand Challenge. A platform for end-to-end development of machine learning solutions in biomedical imaging, 2021. [Online]. Available: https://grand-challenge.org/

[45] The medical image computing and computer assisted intervention society, 2021. [Online]. Available: http://www.miccai2018.org/

9 Authors

Azhar Tursunova is a 3rd-year doctoral student of the specialty Automation and Internet of things of the Department of Artificial Intelligence and Big Data of Al-Farabi Kazakh National University (e-mail: azhar.tursynova1@gmail.com)

Batyrkhan Omarov received his bachelor's and master's degrees from Al-Farabi Kazakh National University, Almaty, Kazakhstan in 2008 and 2010, respectively. In 2019, he received his Ph.D. from Tenaga National University, Kuala Lumpur, Malaysia. His research interests include machine learning, natural language processing, and artificial intelligence in medicine (email: batyahan@gmail.com).

Aivar Sakhipov is the senior lecturer of the Astana IT University (AITU), EXPO Business Center, block C.1., in Nur-Sultan, Kazakhstan (email: aivar.sakhipov@astanait.edu.kz).

Natalya Tukenova is the Head of Department of Information and Communication Technologies at Zhetisu University named after I. Zhansugurov, Zhansugurov 87a, in Taldykorgan, Kazakhstan (email: n.tukenova@zu.edu.kz).

Article submitted 2022-05-31. Resubmitted 2022-08-17. Final acceptance 2022-08-24. Final version published as submitted by the authors.